Probabilistic Secretion of Quanta and the Synaptosecretosome Hypothesis: Evoked Release at Active Zones of Varicosities, Boutons, and Endplates

M. R. Bennett,* W. G. Gibson,# and J. Robinson#
*Neurobiology Laboratory, Department of Physiology, Institute for Biomedical Research, and #School of Mathematics and Statistics, University of Sydney, New South Wales 2006, Australia

ABSTRACT A quantum of transmitter may be released upon the arrival of a nerve impulse if the influx of calcium ions through a nearby voltage-dependent calcium channel is sufficient to activate the vesicle-associated calcium sensor protein that triggers exocytosis. A synaptic vesicle, together with its calcium sensor protein, is often found complexed with the calcium channel in active zones to form what will be called a "synaptosecretosome." In the present work, a stochastic analysis is given of the conditions under which a quantum is released from the synaptosecretosome by a nerve impulse. The theoretical treatment considers the rise of calcium at the synaptosecretosome after the stochastic opening of a calcium channel at some time during the impulse, followed by the stochastic binding of calcium to the vesicle-associated protein and the probability of this leading to exocytosis. This allows determination of the probabilities that an impulse will release 0, 1, 2, . . . quanta from an active zone, whether this is in a varicosity, a bouton, or a motor endplate. A number of experimental observations of the release of transmitter at the active zones of sympathetic varicosities and boutons as well as somatic motor endplates are described by this analysis. These include the likelihood of the secretion of only one quantum at an active zone of endplates and of more than one quantum at an active zone of a sympathetic varicosity. The fourth-power relationship between the probability of transmitter release at the active zones of sympathetic varicosities and motor endplates and the external calcium concentration is also explained by this approach. So, too, is the fact that the time course of the increased rate of quantal secretion from a somatic active zone after an impulse is invariant with changes in the amount of calcium that enters through its calcium channel, whether due to changes consequent on the actions of autoreceptor agents such as adenosine or to facilitation. The increased probability of quantal release that occurs during F1 facilitation at the active zones of motor endplates and sympathetic boutons is predicted by the residual binding of calcium to a high-affinity site on the vesicle-associated protein. The concept of the stochastic operation of a synaptosecretosome can accommodate most phenomena involving the release of transmitter quanta at these synapses.

INTRODUCTION

The evoked secretion of transmitter quanta at synapses that use transmitters acting on ionotropic receptors may be mediated by the influx of calcium through voltage-dependent channels that are in very close proximity to vesicle-associated protein calcium sensors for triggering exocytosis. Such sensors are very likely to include synaptotagmin bound to a complex that includes an N-type calcium channel and the presynaptic protein syntaxin (Südhof, 1995). The combination of a synaptic vesicle bound to the N-terminus of synaptotagmin, together with a syntaxin molecule and a calcium channel, has been termed the synaptosecretosome by O'Connor et al. (1993) (see also Yoshida et al., 1992).

There are both theoretical arguments and physiological evidence supporting the idea that the synaptosecretosome is the release unit for a quantum of transmitter. Partial block, with toxins, of the presynaptic calcium channels involved in evoked quantal release at the active zones of endplates indicates that calcium entry during the opening of a single channel is sufficient to trigger secretion, suggesting that the synaptic vesicle and its calcium sensor protein are in immediate juxtaposition to the channel (Yoshikami et al., 1989). Stanley (1993) observed only one calcium channel opening during the release of a quantum from avian ciliary ganglion terminals; he suggested that the distance between the channel and the calcium sensor protein must be ~25 nm for this to occur. Theoretical calculation of the calcium transient that occurs at the mouth of an open channel shows that discrete peaks of calcium occur immediately adjacent to the channel, and these reach concentrations on the order of 100 μM (Simon and Llinás, 1985); these discrete peaks are now called "calcium domains" (Zucker and Fogelson, 1986). These domains may ensure that a relatively low-affinity calcium-binding site on the calcium sensor can only be activated by the high concentrations of calcium reached in the domain, and therefore exocytosis resulting from the opening of a channel is generally confined to the vesicle in immediate proximity to the channel.

Voltage clamp studies of release in the stellate ganglion of the squid support the notion that high calcium levels generated at active zones during action potentials give rise to release within single nonoverlapping calcium domains within the terminals (Augustine et al., 1991). Given that

Received for publication 23 December 1996 and in final form 16 June 1997.

Address reprint requests to Dr. Max Bennett, Neurobiology Laboratory, University of Sydney, NSW 2006, Australia. Tel.: 61-2-9351-2034; Fax: 61-2-9351-3910; E-mail: maxb@physiol.su.oz.au.

0006-3495/97/10/1815/15 $2.00

calcium channels in ciliary ganglion nerve terminals may occur in clusters in which the channels are separated by ~40 nm (Haydon et al., 1994) and that discrete peaks of calcium have been observed in such clusters in the terminals of the stellate ganglion (Llinás et al., 1995), it is possible that under conditions of sustained depolarization (longer than that provided by an action potential), the calcium that contributes to the activation of a particular calcium sensor in a synaptosecretosome comes from adjacent calcium channels in the channel cluster, in addition to that of the channel in the synaptosecretosome under consideration (Zucker and Fogelson, 1986). This seems to be the case, because release is greater at higher depolarizations where the channel opening probability is higher than at lower voltages that produce the same net calcium current into the terminal (Llinás et al., 1981).

The development of a theory that describes the action of synaptosecretosomes under an action potential at an active zone may allow for an understanding of a number of recent observations on the probability of quantal release at sympathetic varicosities and boutons that possess a single active zone, as well as release at the active zones of motor endplates. These observations include the relatively high multiquantal release at sympathetic varicosities compared with the monoquantal release at the somatic endplate (Bennett, 1994); the linear relationship between the length of an active zone at a somatic endplate and the probability of quantal release there (Bennett et al., 1989); the fourth-power dependence of this probability on external calcium at different sympathetic varicosities and somatic active zones, independent of the their probability in a particular calcium concentration (Bennett and Lavidis, 1989; MacLeod et al., 1994); the time course of the rate of quantal release after an impulse at somatic active zones when errors of detecting double releases are accounted for (Thompson et al, 1995); and finally, the invariance of this time course with substantial changes in the probability of release brought about by such agents as adenosine that mediate inhibition through autoreceptors (Bennett et al., 1991; Van der Kloot, 1988). In the present work, an analysis is provided of the function of the synaptosecretosome during a nerve impulse. This involves consideration of the stochastic opening of the channel under the impulse, the subsequent diffusion of calcium to the calcium sensor protein, and the stochastic binding of calcium to the different affinity sites on the protein followed by the stochastic event of exocytosis itself.

METHOD

Calcium concentration due to the opening of a single channel

The model used for determining the calcium concentration is essentially the same as that used in our previous work on spontaneous release (Bennett et al., 1995), which in turn was based on earlier work by other authors (Fogelson and Zucker, 1985; Parnas et al., 1989). The result for the calcium concentration at a point (x, y) a distance $r = \sqrt{x^2 + y^2}$ from the center of a single channel is

$$c(r, t) = \frac{A}{1 + B}\frac{2}{\pi^{3/2}} \int_0^t \frac{1}{\sqrt{\mathcal{D}(t-\tau)[\mathcal{D}(t-\tau) + 2\sigma^2]}} e^{-r^2/[\mathcal{D}(t-\tau)+2\sigma^2]} g(\tau)|i(\tau)|\mathrm{d}\tau \quad (1)$$

Here $|i(t)|$ is the magnitude of the single-channel current $i(t)$; $g(y) = 1$ when the channel is open and is zero otherwise; $\mathcal{D} = 4D/(1 + B)$, where D is the diffusion constant for aqueous solution and B is the ratio of bound to free calcium due to buffering; σ is the standard deviation of the Gaussian channel profile; and A is a constant. (If $i(t)$ is measured in pA, then taking $A = 5.20$ gives $c(r, t)$ in μM.) The calcium concentration can now be found by using numerical integration in Eq. 1; in the special case where $\sigma = 0$ and $i(t)$ is constant, Eq. 1 can be evaluated explicitly in terms of incomplete gamma functions (Bennett et al., 1995).

Distribution of open and closed times for a single channel

A single calcium channel will open and close stochastically, with its opening and closing probabilities determined by the membrane potential $V = V(t)$. The simplest scheme involves only two states, C (closed) and O (open), and is governed by the kinetic scheme

$$C \underset{k_{-1}}{\overset{k_1}{\rightleftarrows}} O \quad (2)$$

involving the two rate parameters $k_1 = k_1(t) = k_1(V(t))$ and $k_{-1} = k_{-1}(t) = k_{-1}(V(t))$. A more appropriate model of the channel would incorporate at least a three-state scheme (Jones and Marks, 1989a, b) or use a more detailed model of the calcium gating mechanism (Llinás et al., 1981). However, for N-type calcium channels operating in the low-p_0 mode (see below), the available experimental data (Delcour et al., 1993) are insufficient to justify this increased complexity, and the above scheme gives a good fit. The rate parameters are assumed to depend on the potential via the Boltzmann-type expressions (Hille, 1992, Ch. 10)

$$k_1 = a_1 \exp(b_1 V) \quad (3)$$

$$k_{-1} = a_{-1} \exp(b_{-1} V) \quad (4)$$

where a_1, b_1, a_{-1}, b_{-1} are constants, independent of the potential.

The opening and closing of channels are (nonhomogeneous) Poisson processes, with rates k_1 and k_{-1}, respectively. It follows (Clay and DeFelice, 1983) that the closed

times T_c have density function

$$\rho_c(t) = k_1(t)\exp\left(-\int_0^t k_1(\tau)d\tau\right) \quad (5)$$

and the open times T_o have density function

$$\rho_o(t) = k_{-1}(t)\exp\left(-\int_0^t k_{-1}(\tau)d\tau\right) \quad (6)$$

If the potential is constant, these are simple exponential distributions, and the average closed and open times are $E(T_c) = 1/k_1$ and $E(T_o) = 1/k_{-1}$, respectively.

The single-channel current

The single-channel current $i(t)$ also depends on the membrane potential $V(t)$: $i(t) = i(V(t))$. The Goldman-Katz-Hodgkin (GHK) equation (Hille, 1992, Ch. 13) predicts the form

$$i(t) = \kappa \frac{V}{1 - e^{0.075V}} \quad (7)$$

where κ is a constant that does not depend on the voltage, and this form can be used in calculations (Bertram et al., 1996). However, as observed by Llinás et al. (1981), this constant-field approximation tends to overestimate the current at large depolarizations, and this is also found when Eq. 7 is fit to the N-type calcium channel currents measured by Delcour et al. (1993). Llinás et al. (1981) propose an alternative formula that involves the internal and external calcium concentrations, but in the present context the simple modification

$$i(t) = \bar{\kappa} \frac{V - \bar{V}}{1 - e^{0.075(V - \bar{V})}} \quad (8)$$

where $\bar{\kappa}$ and $\bar{V}$ are constants, is sufficient to give a good fit to the experimental data (see below).

Stochastic opening of a single calcium channel under a step potential change

Let the potential have the time course

$$V = \begin{cases} V_1 & \text{if } 0 < t < t_{end} \\ V_0 & \text{otherwise} \end{cases} \quad (9)$$

where V_1 and V_0 are constants and t_{end} is a given time (Fig. 1). If V_0 is sufficiently negative, there will be negligible probability of spontaneous openings before the potential step, so it is assumed that the channel is closed at $t = 0$. In the interval $(0, t_{end})$ the channel opening and closing are governed by the parameters $k_1(V_1)$ and $k_{-1}(V_1)$; in a simulation, one generates random deviates r_i, uniform on [0, 1], and then the closed times are $|\log_e r_i|/k_1(V_1)$ and the open times are $|\log_e r_i|/k_{-1}(V_1)$. Thus the channel may not open at all, or it may undergo multiple openings and closings in $(0, t_{end})$; during each opening the current flow is $i_1 = i(V_1)$, as given by Eq. 8. One special case to note is where the channel is open at $t = t_{end}$; its closing time is then governed by $k_{-1}(V_0)$ and the current jumps from $i_1 = i(V_1)$ for $t < t_{end}$ to $i_0 = i(V_0)$ for $t > t_{end}$, giving the tail current. Some of these possibilities are illustrated in Fig. 1.

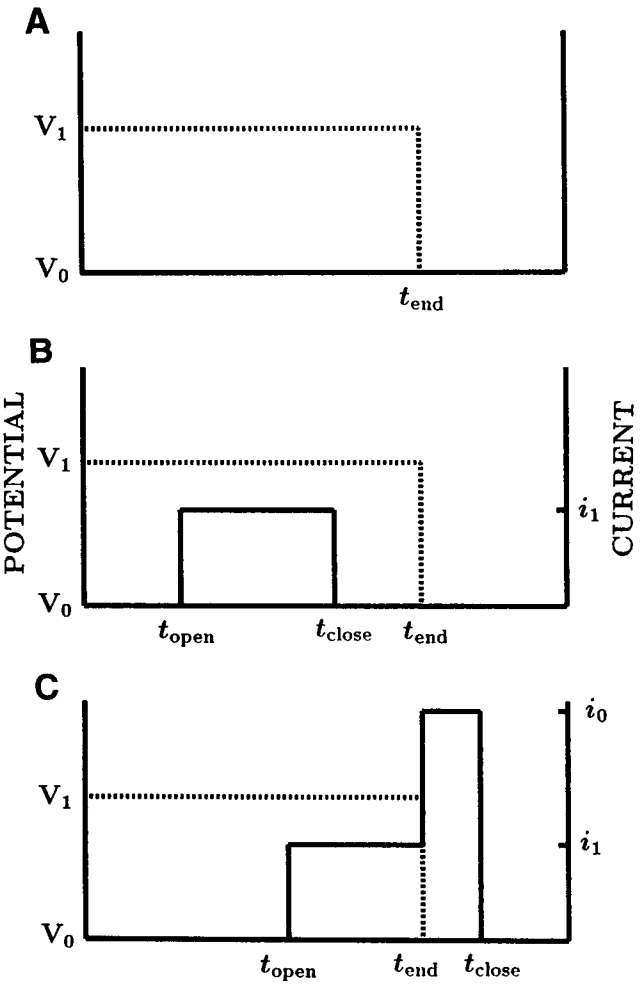

FIGURE 1 Three cases of currents in a channel related to the time of its opening during a step change in the membrane potential. The broken line shows that the voltage increases from V_0 to V_1 at time $t = 0$ and then reverts to V_0 at $t = t_{end}$. The continuous line shows the single-channel current, beginning at t_{open} and ending at t_{close}. The three cases shown are (*A*) the channel does not open; (*B*) the channel opens and closes within the voltage step; (*C*) the channel opens in the voltage step and closes after the step.

Stochastic opening of a single calcium channel under an action potential

The membrane potential $V(t)$ during an action potential is found by solving the Hodgkin-Huxley equations. The single-channel current $i(t)$ and the channel opening and closing

rates $k_1(t)$ and $k_{-1}(t)$ are now all functions of $V(t)$ and can be found from Eqs. 8, 3, and 4. The channel opening and closing times must now be calculated by using the densities in Eqs. 5 and 6. Assuming the channel is initially closed, one first finds an opening time s_i by solving (Clay and DeFelice, 1983)

$$\int_0^{s_i} k_1(\tau)\mathrm{d}\tau = |\log_e r_i| \tag{10}$$

where r_i is a random deviate uniformly distributed on [0, 1]. The subsequent closing time is then found by solving a corresponding equation involving k_{-1}. Because multiple openings of the same calcium channel under a single action potential are rare, they are omitted from the calculations in this paper.

Stochastic binding of calcium to the exocytotic vesicle protein

It is assumed that four sites on a particular vesicle-associated protein must each bind a calcium ion, and then a further conformational change occurs for exocytosis of a vesicle to be triggered. The simplest case is when all of the sites have the same affinity, in which case the kinetic scheme is

$$S_0 \underset{\nu_1}{\overset{4\mu_1}{\rightleftarrows}} S_1 \underset{2\nu_2}{\overset{3\mu_2}{\rightleftarrows}} S_2 \underset{3\nu_3}{\overset{2\mu_3}{\rightleftarrows}} S_3 \underset{4\nu_4}{\overset{\mu_4}{\rightleftarrows}} S_4 \overset{\beta}{\rightarrow} S_{\mathrm{ex}} \tag{11}$$

where S_i, $i = 1, \ldots, 4$, denotes the state with i sites occupied; S_{ex} denotes the state with four sites occupied after the conformational change; $\mu_i(t)$ ($\nu_i(t)$) are the rates of attachment (detachment) of a calcium ion at the ith step; and $\beta(t)$ is the rate for the final step. It is then easy to write down a set of coupled differential equations for the probabilities $P_i(t)$ that the system is in state i at time t (see the Appendix); the rate of exocytosis is then $\mathrm{d}P_{ex}/\mathrm{d}t$, and the probability of exocytosis occurring is the asymptotic value of $P_{ex}(t)$ for large t. The attachment rates μ_i are taken to be proportional to the calcium concentration at the position of the vesicle-associated protein, and the detachment rates ν_i are taken to be constants, independent of time:

$$\mu_i = k_i^a c(r, t); \quad \nu_i = k_i^d; \quad i = 1, \ldots, 4 \tag{12}$$

and the conformational change rate β is taken to be a time-independent constant. A further simplification is to assume no cooperativity in binding or unbinding, in which case $k_i^a = k^a$ and $k_i^d = k^d$, $i = 1, \ldots, 4$.

A more general scheme involves binding sites of different affinities; for the case where there are two sites of each type (designated H for high affinity and L for low affinity), the appropriate kinetic scheme is

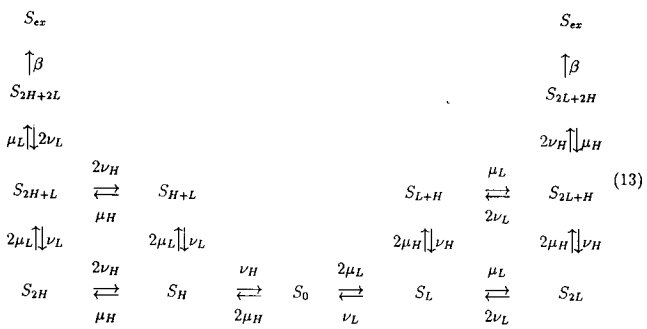

(13)

The corresponding set of differential equations for the binding probabilities is given in the Appendix. Again, the attachments rates μ_H and μ_L are taken to be proportional to the calcium concentration at the position of the vesicle-associated protein:

$$\mu_H = k_H^a c(r, t); \qquad \mu_L = k_L^a c(r, t) \tag{14}$$

and the detachment rates ν_L and ν_H are taken to be constants, independent of time:

$$\nu_H = k_H^d; \qquad \nu_L = k_L^d \tag{15}$$

Facilitation

Suppose an action potential initiated at time $t = 0$ (the conditioning impulse) is followed at time $t = t_1$ by a second impulse (the test impulse). The facilitation of the second response is defined as

$$\text{facilitation} = \frac{P_{ex}[\text{second impulse}]}{P_{ex}[\text{first impulse}]} \tag{16}$$

This is calculated (single affinity case; see Table 2) by first solving Eq. 19 for the probabilities $P_i(t)$, $i = 0, \ldots, 4$, and $P_{ex}(t)$ after the first impulse, using the initial conditions given by Eq. 20 and then using these values at $t = t_1$ as the initial conditions for the second impulse; that is, Eq. 19 is solved again, but now with the initial conditions

$$P_i(t_1+) = P_i(t_1-), \quad i = 0, \ldots, 4 \tag{17}$$

$$P_{ex}(t_1+) = 0 \tag{18}$$

and $P_{ex}[\text{second impulse}] = P_{ex}(t \gg t_1)$ is now calculated. ($P_{ex}[\text{first impulse}]$ is calculated as $P_{ex}(t_1-)$.) The condition given by Eq. 18 means that if the vesicle undergoes exocytosis after the first impulse, then it is not available for a second release under the second impulse. If this restriction is not imposed, then the appropriate expression for the probability of a release as a result of the second impulse is $P_{ex}[\text{second impulse}]/(1 - P_{ex}[\text{first impulse}])$, where $P_{ex}[\text{second impulse}]$ is calculated as described above. These considerations are readily extended to the the dual-affinity case (see Table 2).

Determination of parameter values for the calcium channels and calcium diffusion

The numerical values of the parameters used in the calculations involving the opening of calcium channels and the diffusion of calcium from these to the vesicle-associated protein are listed in Table 1.

The channel gating kinetics were fitted to experimental data for N-type calcium channels operating in the low-p_0 mode (Delcour et al., 1993). N-type channels were chosen for the modeling process, as they are the channels mediating the calcium influx that triggers exocytosis in the majority of synapses of interest in the present study, namely amphibian neuromuscular junctions (Katz et al., 1995), sympathetic neuromuscular junctions (Wright and Angus, 1996), and autonomic preganglionic synapses (Haydon et al., 1994). The single exponentials for k_1 and k_{-1}, Eqs. 3 and 4, gave good fits to the experimental data of Delcour et al. (1993). For the single-channel current $i(t)$, a least-squares fit to the GHK form, Eq. 7, gave a poor fit and, in particular, predicted far too large a current at small depolarizations (Fig. 2, *broken line*); the modified form, Eq. 8, gave a much better fit (Fig. 2, *solid line*).

Solution of the Hodgkin-Huxley equations gives the impulse shown in Fig. 3 *A*. The variation in the rate constants k_1 and k_{-1} during the potential changes accompanying this impulse, calculated from Eqs. 3 and 4, is shown in Fig. 3, *B* and *C*, respectively. The forward rate constant k_1 is relatively large during the main depolarization phase of the impulse, between ~1.0 ms and 2.0 ms (Fig. 3 *B*), determining that the histogram of opening times will follow this potential dependence; the reverse rate constant k_{-1} has a behavior that is to some extent the reciprocal of that of k_1 (Fig. 3 *C*). The magnitude of the calcium flux through a calcium channel that is open for the duration of the impulse is calculated using Eq. 8 (shown in Fig. 3 *D*). It is almost the inverse of the impulse, declining from a value of ~1.5 pA at the resting potential to less that 0.2 pA at the peak of the impulse, and then increasing to reach a maximum of ~2 pA at the peak of the afterhyperpolarization (Fig. 3 *D*).

Consideration must be given to the calcium affinity values of the different binding sites on the vesicle-associated protein before calculations can be made of the probability of exocytosis due to an impulse. The K_d values for calcium-mediated events that are probably involved in exocytosis range from 2.6 μM to 100 μM (see Discussion). We have therefore chosen K_d in this range, as shown in Table 2. As the attachment rates (k^a) are ~15 × 10^6 M^{-1} s^{-1} in successful descriptions of the experimental data for exocytosis from chromaffin cells (Heinemann et al., 1994) and bipolar cells (Heidelberger et al., 1994), this value has been chosen for k^a in the present work, thus fixing k^d for a given K_d (Table 2). The effect of varying k^a on the probability of exocytosis is considered further below (see Fig. 8) for the case in which all four binding sites are taken to have the same affinity, referred to as the "standard single affinity" case (Table 2). Consideration is also given to the case in which the binding sites have different affinities; in particular, a "standard dual-affinity" case, in which two sites have higher affinity than in the single-affinity case and two have lower affinity, is used in a number of calculations (Table 2). The dual-affinity case is important when considering the possibility that F1 facilitation is due to residual Ca^{2+} binding to a site on the vesicle-associated protein (Yamada and Zucker, 1992; see Fig. 6 below). Finally, some consideration is given to the effects of using the affinity values adopted for describing secretion from chromaffin cells and bipolar cells on the probability of exocytosis (Table 2; see Fig. 7).

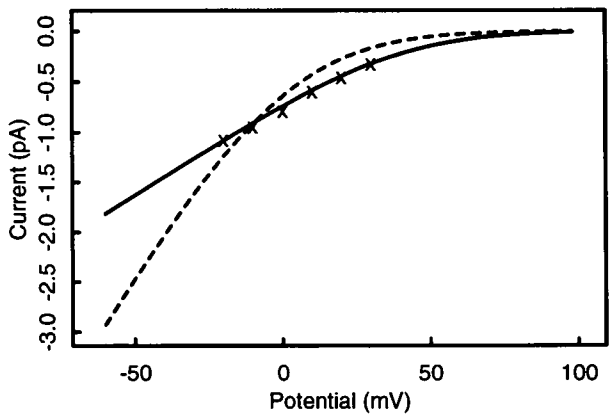

FIGURE 2 Least-squares fits to the measured currents for an N-type calcium channel at different voltages. The crosses are the measured currents from Delcour et al. (1993), the broken line is the fit using Eq. 7, and the solid line is the fit using Eq. 8.

TABLE 1 Values of the parameters used in the numerical calculations involving calcium channel kinetics and calcium diffusion

Quantity	Symbol	Value	Reference
Calcium diffusion coefficient (Eq. 1)	D	0.6 μm^2 ms^{-1}	Fogelson and Zucker (1985)
Bound to free calcium ratio (Eq. 1)	B	100	Brinley (1978)
Channel spatial profile (Eq. 1)	σ	1 nm	Aharon et al. (1994)
Channel opening rate parameters (Eq. 3)	a_1	0.102 ms^{-1}	Delcour et al. (1993)
	b_1	0.046 mV^{-1}	Delcour et al. (1993)
Channel closing rate parameters (Eq. 4)	a_{-1}	1.256 ms^{-1}	Delcour et al. (1993)
	b_{-1}	−0.022 mV^{-1}	Delcour et al. (1993)
Single-channel current parameters (Eq. 8)	$\bar{V}$	37.56 mV	Delcour et al. (1993)
	$\bar{\kappa}$	0.0186 pA mV^{-1}	Delcour et al. (1993)
Channel-vesicle distance		20 nm	See text

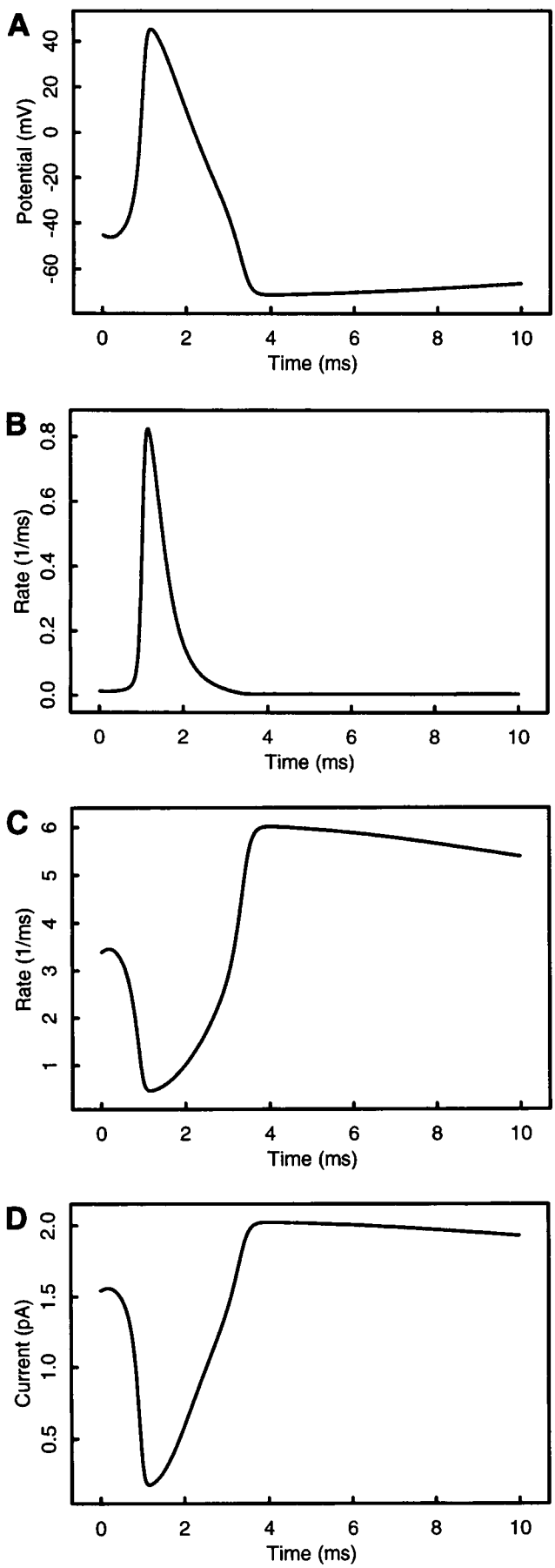

RESULTS

Probability of exocytosis at a synaptosecretosome

The synaptosecretosome has been defined in the Introduction as a synaptic vesicle together with its vesicle-associated proteins and a calcium channel, the latter being situated ~20 nm away from the protein that acts as the calcium sensor. The active zones considered in this analysis are taken as possessing N-type calcium channels. In this section, the probability of exocytosis from a single synaptosecretosome, in isolation from the influences of calcium entering at other synaptosecretosomes, is considered.

A histogram of times at which a channel opens under an action potential can be calculated by using Eq. 10. Fig. 4 *A* shows the results of a simulation using 10,000 impulses, where each impulse has the form shown in Fig. 3 *A*. In 4638 cases there was an opening during the impulse (giving an opening probability of 0.464), with most openings occurring in the period between 1.0 ms and 2.0 ms, that is over the same period as the occurrence of relatively large values in k_1 (Fig. 3 *B*), which is reflected in the fact that the histogram has a shape similar to that of the graph of k_1. The corresponding calculation of the channel closing times, using Eq. 10 with $k_1(\tau)$ replaced by $k_{-1}(\tau)$, yields a histogram of channel open durations (Fig. 4 *B*) which shows that channels may remain open for up to ~2.5 ms. However, the duration of most open times is much less (mean = 0.831 ms in Fig. 4 *B*), because the reverse rate parameter k_{-1} (Fig. 3 *C*) peaks very shortly after the most likely opening times.

For a given pair of calcium channel opening and closing times during an impulse, Eq. 1 allows the calculation of the calcium concentration at the sensor protein in a synaptosecretosome after diffusion from the open channel. Moderate concentrations occur when the channel is open during the early part of the impulse, lower concentrations occur when the open time is mainly during the peak of the impulse, and the largest concentrations are reached when the channel is open during the repolarization phase of the impulse.

Fig. 5 shows the exocytosis rate from a synaptosecretosome due to a rise in calcium concentration at the four binding sites on the calcium-sensor protein, having the standard single affinity (Table 2), after the opening of the calcium channel in the synaptosecretosome during a nerve impulse. The first case chosen for illustration is where the calcium channel always opens at 1.0 ms after the beginning

FIGURE 3 Behavior of a calcium channel during an impulse. (*A*) The time course of the impulse according to the solution of the Hodgkin-Huxley equations. (*B*) The time dependence of the forward rate constant k_1 during the Hodgkin-Huxley impulse, according to Eq. 3. (*C*) The time dependence of the reverse rate constant k_{-1} during the Hodgkin-Huxley impulse, according to Eq. 4. (*D*) The time dependence of the magnitude of the ionic current, $|i(t)|$, through a single calcium channel during the Hodgkin-Huxley impulse, given that the channel is open throughout the impulse, according to Eq. 8.

TABLE 2 Values of the rate constants for calcium binding

Scheme	k^a (10^6 M^{-1} s^{-1})	k^d (s^{-1})	K_d (μM)	β (s^{-1})	Reference
"Standard single affinity"	15	750	50	2000	See text
"Standard dual affinity"					See text
High affinity	15	75	5	2000	
Low affinity	15	1500	100	2000	
Chromaffin (slow)	19	130	7	100	Heinemann et al. (1994)
Chromaffin (fast)	14	130	9	1000	Heinemann et al. (1994)
Bipolar	14	2000	143	3000	Heidelberger et al. (1994)
		800	57		
		320	23		
		128	9		

k^a is the attachment rate and k^d is the detachment rate; $K_d = k^d/k^a$ is the dissociation constant; and β is the rate constant for the conformational change after four calcium ions are bound. The "standard single-affinity" scheme has four binding sites of the same affinity. The "standard dual-affinity" scheme has two high-affinity binding sites and two low-affinity binding sites. The chromaffin (slow) and chromaffin (fast) schemes are fits to two different classes of cells. The bipolar scheme has four sites of the same affinity, but the unbinding is cooperative, with the rate constant decreasing by a factor of 0.4 for each successive calcium ion.

of the impulse and has an open duration of 2.0 ms (Fig. 5 *A*); the probabilities $P_k(t)$ that the calcium sensor protein has bound k calcium ions by time t, $k = 0-4$, given the calcium changes in Fig. 5 *A*, are calculated using Eq. 19. The exocytosis rate from the synaptosecretosome, $dP_{ex}(t)/dt$, is then as shown in Fig. 5 *C*.

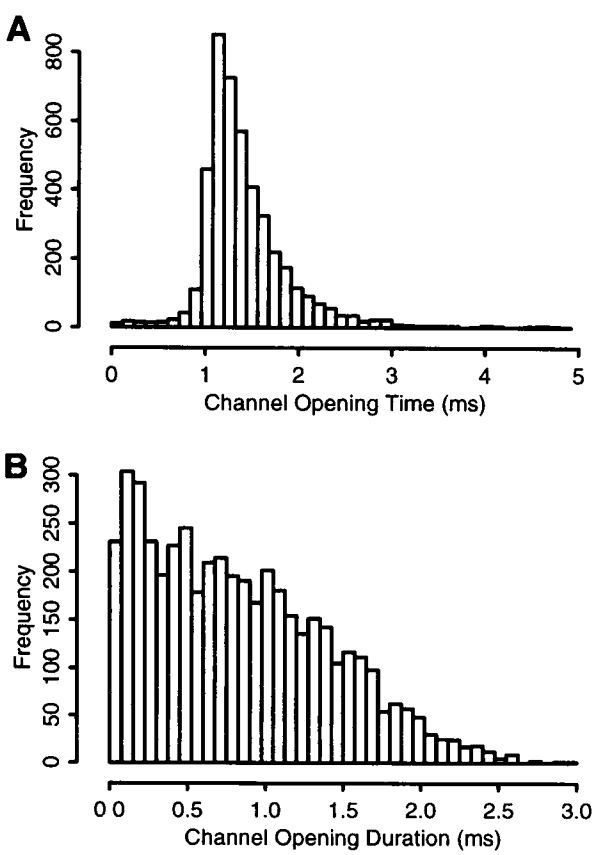

FIGURE 4 Histograms of the times at which a calcium channel opens (*A*) and the duration of the open time (*B*) for a channel under the impulse of Fig. 3 *A*. A total of 4638 openings were obtained for a run of 10,000 impulses.

This calculation is now extended to the case in which the calcium channel in the synaptosecretosome opens and closes stochastically during an impulse, according to the kinetic scheme of Eq. 2 (Fig. 5 *C*, *D*). It should be noted that the peak of the exocytosis rate occurs after the peak of the impulse, as is observed experimentally for transmitter release in the squid stellate ganglion (Llinás et al., 1982).

Changes in the probability of exocytosis from a synaptosecretosome

The time course of the rate of exocytosis after an impulse at the amphibian motor nerve terminal is invariant under a number of procedures that greatly change exocytosis at the terminal. These include an increase in the external calcium concentration and facilitation, both of which increase exocytosis (Datyner and Gage, 1980), and the action of adenosine, which decreases exocytosis (Van der Kloot, 1988). These observations can be accommodated by a scheme in which two of the binding sites on the calcium sensor protein have a relatively high affinity for calcium and the other two have relatively low affinities (the "standard dual-affinity" case of Table 2; see also Yamada and Zucker, 1992). Calculations using 1000 impulses, with the external calcium concentration reduced to one-half of the normal level, showed that the average peak rate is decreased sixfold over this concentration range (from 0.0124 ms^{-1} to 0.0020 ms^{-1}), but when the rates are normalized to their peak values, the time courses in the different calcium concentrations are very similar.

Simulations were also done for the case in which the probability of opening of a calcium channel in the synaptosecretosome during an impulse was decreased (by reducing a_1 in Eq. 3 to one-half its normal value), as is thought to be the case for the action of adenosine (Bennett and Ho, 1991); this led to a 40% decrease in the peak rate of exocytosis from the synaptosecretosome, but with no change in the time course of the normalized exocytosis rate. Finally, simulations were carried out to see if the increase in

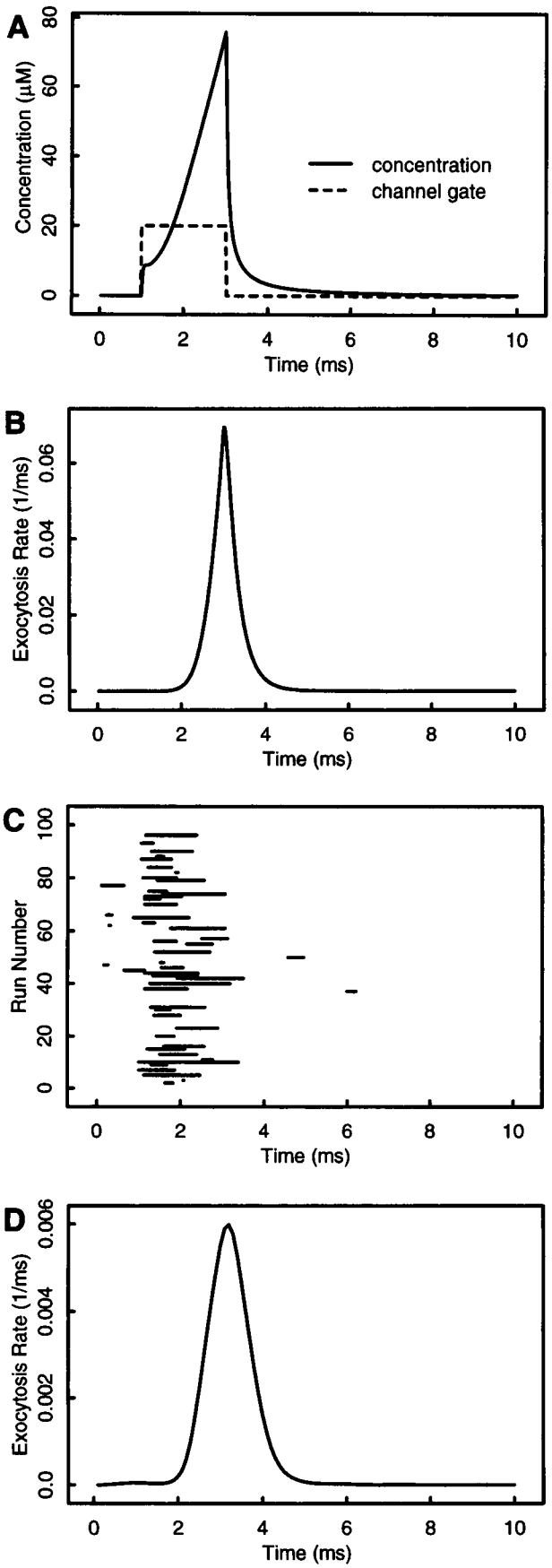

the rate of exocytosis due to a test impulse 10 ms after a conditioning impulse caused any change in the time course of the rate of exocytosis. The calculation again used 1000 impulses (and the standard dual-affinity rate constants in Table 2). The results show an invariance in the time course of the exocytosis rate, although there is a 12% increase in the peak rate after the test impulse compared with that after the conditioning impulse.

The average probability of quantal release decreases with a decrease in the external calcium concentration, and this more closely approximates a fourth-power relationship as the calcium is lowered (Dodge and Rahamimoff, 1967; Bennett and Lavidis, 1989; Augustine et al., 1985), whereas facilitation decreases with an increase in the calcium concentration (Rahamimoff, 1968). Simulations show that for a decrease in the external calcium concentration, the average probability of exocytosis more closely approximates a four-fold cooperative relationship with calcium (Fig. 6 *A*), and simulations involving a test impulse 10 ms after a condition impulse show that the facilitatory effect declines as the external calcium concentration increases (Fig. 6 *B*), as is observed experimentally.

Although the above calculations have used the dual affinity for the calcium sensor and protein, there is very little difference in the probability of exocytosis by a single impulse between the dual-affinity case and the single-affinity case, the frequency distribution of this probability being only marginally greater for the dual-affinity case over that of the single-affinity case. Some of the effects of changes in the affinities on the probability of exocytosis from a synaptosecretosome over two impulses are shown in Fig. 7, where results are given for each of the sets of affinities listed in Table 2. Cases 1 and 2, for the standard single and dual affinities, show very little difference in the probability of exocytosis, although the dual case shows substantially greater facilitation (indicated by the *open bars*). Case 3 for the slow exocytosis from chromaffin cells is similar to Case 2, whereas the affinities for the fast exocytosis from chromaffin cells (Case 4) give very high probabilities and facilitation. The bipolar cell calcium affinities (Case 5) give a high probability of exocytosis but little facilitation.

FIGURE 5 Probability of exocytosis for a vesicle opening under an impulse. The vesicle, with its calcium-sensitive vesicle-associated proteins, is located 20 nm from a calcium channel (together these comprise the synaptosecretosome). (*A*) The change in calcium concentration at the calcium sensor (*solid line*), obtained by evaluating Eq. 1 for the particular case of a channel opening at 1.0 ms and closing at 3.0 ms, as depicted by the broken curve. (*B*) The rate of exocytosis (dP_{ex}/dt) of the vesicle for the case illustrated in *A*, using the standard single-affinity rate constants (Table 2). (*C*) The times of opening and closing of a calcium channel during 100 different impulses that resulted in 50 openings during the time interval 0–10 ms; the length of each line gives the open time for that run. (These are part of a simulation involving 1000 impulses in which 434 openings occurred, the remainder giving no opening during the interval 0–10 ms.) (*C*) The corresponding rate of exocytosis when the channel opens stochastically; the graph shows the average of 1000 impulses, which resulted in 434 channel openings.

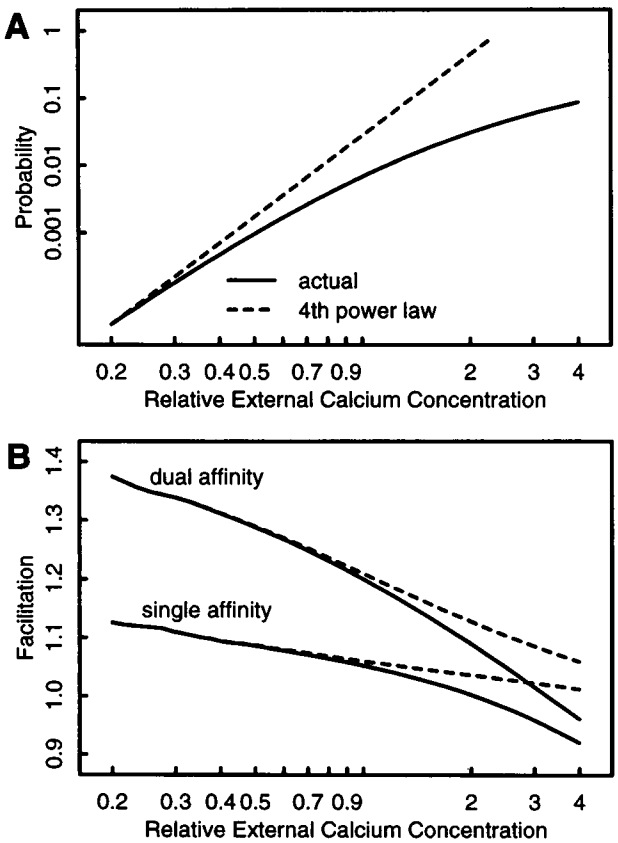

FIGURE 6 The relationship between the calcium concentration on the one hand and both the probability of exocytosis at a synaptosecretosome and the facilitated probability of exocytosis. The results shown are the average of 1000 simulations at each calcium concentration, using the standard dual-affinity rate constants (Table 2). (*A*) The probability (*log scale*) of exocytosis for different calcium concentrations, after a Hodgkin-Huxley impulse. The calcium concentration (*log scale*) is expressed as a proportion of the normal calcium concentration; the solid line is the result of the simulations, and the broken line is the probability according to a fourth-power law. (*B*) The facilitated exocytosis due to a test impulse 10 ms after a conditioning impulse, where both are Hodgkin-Huxley action potentials. The ordinate gives the ratio of the probability of exocytosis after the test impulse to the probability of exocytosis after the conditioning impulse only; the abscissa is on a log scale. The solid curve gives the facilitation, assuming that the vesicle cannot release after the test impulse if it already released under the conditioning impulse; the broken line gives the ratio of probabilities without this restriction (see the discussion of facilitation in the Methods section above). Also shown (*lower curves*) are the corresponding results found with the standard single-affinity scheme (Table 2).

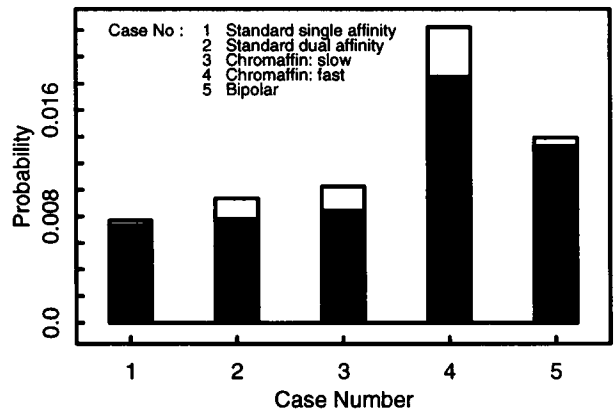

FIGURE 7 The probability of exocytosis at a synaptosecretosome during 1000 Hodgkin-Huxley impulses for different combinations of the affinity of the calcium-binding sites on the synaptic vesicle-associated protein for normal calcium concentration. The graph shows the results for each of the five cases listed in Table 2. The heights of the solid bars give the probability of exocytosis under a conditioning impulse, and the heights of the open bars give the probability of exocytosis under a test impulse 10 ms after the conditioning impulse.

The probability of exocytosis from a synaptosecretosome depends critically not only on these affinities for calcium binding of the calcium sensor, but also on the distance between the sensor and the calcium channel, as has been detailed previously for spontaneous quantal secretion (Bennett et al., 1995). The relationship between changes in the distance between the calcium channel and the calcium sensor on the one hand and changes in the affinity of the calcium-binding sites in the sensor was therefore investigated. Fig. 8 shows that for a particular set of single affinities, whether low or high, the probability of exocytosis increases continually with a decrease in this distance.

Exocytosis from multiple synaptosecretosomes in active zones

Active zones possess synaptosecretosomes in different numbers and in different geometrical arrays, as reviewed in Bennett et al. (1995): the synaptosecretosomes in varicosities of the autonomic neuromuscular junction appear to be randomly distributed in the prejunctional membrane, whereas those at active zones in the somatic neuromuscular junction are arranged on a line; in the case of active zones in boutons on autonomic ganglion cells, the synaptosecretosomes appear to be arranged on a grid. If the action of the transient high calcium concentration that occurs around an open channel of a synaptosecretosome (constituting the calcium domain) is confined to the calcium sensor protein in that synaptosecretosome, then the different synaptosecretosomes in an active zone act independently of each other. Determination of the probability of $k = 0, 1, 2, 3$ or more exocytotic events on the arrival of an impulse at the active zone then involves solving the binomial equation, where n is equal to the number of synaptosecretosomes in the active zone and p is the average probability of exocytosis from a synaptosecretosome. The results of such calculations for the case of the random distribution of synaptosecretosomes (the varicosity case), synaptosecretosomes on a grid (the bouton case), and synaptosecretosomes on the line (the somatic motor nerve terminal case) are shown in Fig. 9 for the single-affinity condition (Table 2). These show that at the active zone of an amphibian somatic neuromuscular junction, there is an average probability for secretion of ~0.2, with very few double quantal releases occurring (Fig. 9 *C*);

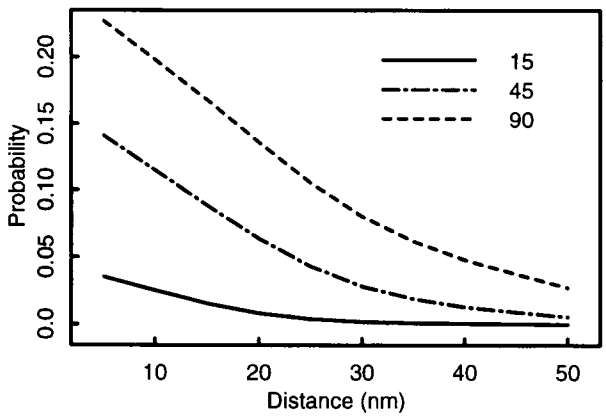

FIGURE 8 The effect of changing the distance between the calcium channel and the calcium sensor in the synaptosecretosome on the probability of exocytosis. Single-affinity binding is used, in which the reverse rate constant is fixed at $k^d = 750\ s^{-1}$ and the forward rate constant has value $k^a = 15$ (*solid curve*), 45 (*dot-dash curve*), and 90 (*broken curve*) $\times\ 10^6\ M^{-1}\ ms^{-1}$.

as this junction has ~500 active zones, the average quantal content of the endplate potential in a calcium of 1.8 mM should be 100, which is approximately the case (Bennett and Fisher, 1977). At the autonomic neuromuscular junction, such as that of sympathetic nerve terminals in the mouse vas deferens, the active zone releases on average ~60% of occasions, with ~35% of these involving either a double or triple quantal release (Fig. 9 *A*), as is observed when recordings are made from single varicosities at these junctions (Bennett, 1994). Finally, at boutons on autonomic ganglion cells, there is on average a release of quanta on ~45% of occasions, with ~25% of these involving multiquantal release (Fig. 9 *B*). It is not known at present what the frequency of multiquantal releases is at these boutons, as it appears that one exocytotic event is sufficient to saturate the postsynaptic receptor patch (Bennett et al., 1997), so that a quantal analysis at the single bouton level is not possible.

Facilitation of exocytosis from multiple synaptosecretosomes in active zones

The temporal changes in increased efficacy of quantal release that occurs at a nerve terminal when a test impulse follows at different intervals after a conditioning impulse have been characterized for motor nerve terminals and, indeed, for other terminals (Magleby and Miller, 1982). These are F1 facilitation (with a time constant of ~30 ms), F2 facilitation (with a time constant of ~500 ms), augmentation (with a time constant of ~5 s), and after a conditioning train of impulses, posttetanic potentiation (with a time constant of ~120 s). The condition of F1 facilitation arises immediately from the properties of the high-affinity calcium-binding site of the calcium sensor in the synaptosecretosome for the dual-affinity case (Table 2). Calculations show that if a test impulse occurs some 10 ms after the conditioning impulse, there will be a higher probability that

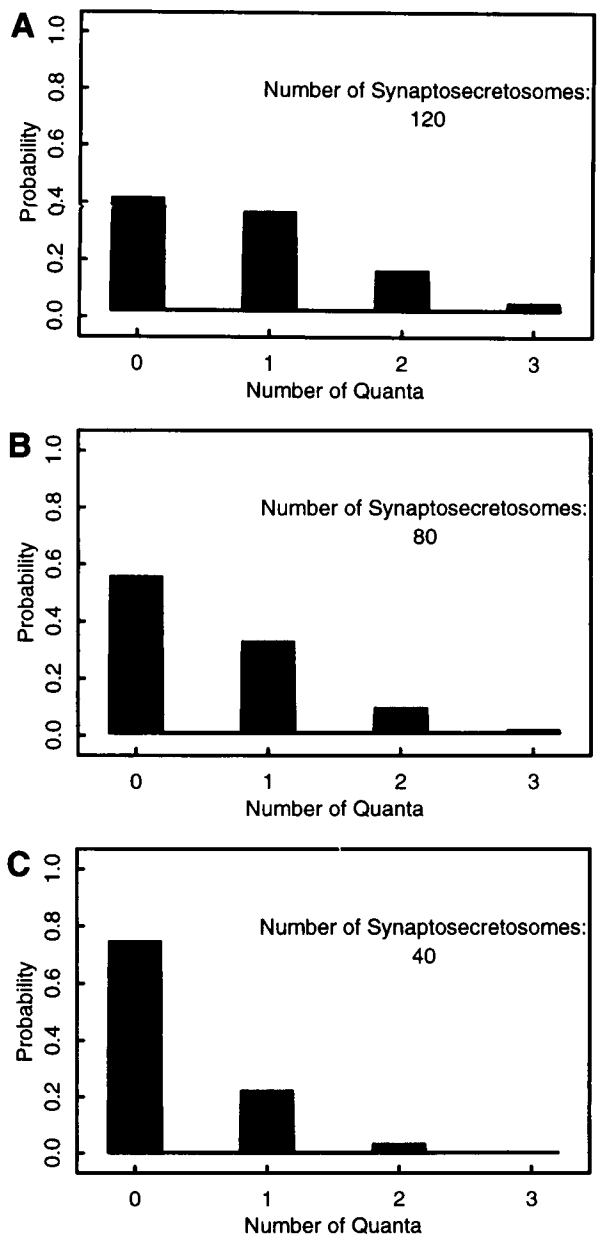

FIGURE 9 The probability p_k of a single Hodgkin-Huxley impulse leading to the exocytosis of k vesicles from n independent synaptosecretosomes when the probability of each exocytosis is p. The value $p = 0.00731$ is calculated using the standard single-affinity rate constants (compare Fig. 7 Case 1), and the probabilities are found from the binomial distribution as $p_k = b(k; n, p)$. (*A*) Varicosity case, for which the assumption of a two-dimensional random distribution of synaptosecretosomes leads to the estimate $n = 120$. (*B*) Bouton case, for which the assumption of a two-dimensional regular-grid array of synaptosecretosomes leads to the estimate $n = 80$. (*C*) Motor nerve terminal case, for which the assumption of a one-dimensional regular spacing of synaptosecretosomes leads to the estimate $n = 40$.

all four calcium binding sites on the sensor will be occupied during the test impulse as a consequence of the residual number of high-affinity sites still occupied by calcium ions at the time of the test impulse. The result is an increased probability of exocytosis for the test impulse, according to

the solution of Eqs. 21–23. The probability of k exocytotic events occurring at an active zone that possesses 40 independent synaptosecretosomes (such as the somatic neuromuscular junction) for the test and conditioning impulses can then be calculated in the same way as was done in relation to Fig. 9. The results show that there is an increase in the number of occasions on which an exocytotic event occurs for the test impulse after the conditioning impulse, which is similar to what is observed during facilitation at the active zones of motor nerve terminals (Bennett and Lavidis, 1989).

DISCUSSION

F1 facilitation and the calcium sensor protein

The question arises as to the correct modeling of the calcium sensor protein. The idea that at least four sites must bind calcium ions on the sensor has been established by determination of the calcium sensitivity of release at single varicosities (MacLeod et al., 1994) and active zones of endplates (Bennett and Lavidis, 1989), following the pioneering work of Dodge and Ramamimoff (1967). These studies obtained a Hill coefficient for release of ~4, which was shown by Augustine et al. (1985) to be due most likely to the dependence of the release sensor on binding four calcium ions. Yamada and Zucker (1992) pointed out the necessity of rapid equilibration of calcium binding to a low-affinity site on the sensor if the sensor was to be able to respond selectively in the release process to just the transient high calcium in the calcium domain and to be able to terminate release soon after the calcium channel has opened. These authors also pointed out the necessity of the sensor possessing a slow equilibrating site with high affinity if the phenomenon of F1 facilitation was to occur. In this latter case, calcium entering during a conditioning impulse then leaves one of the sensor binding sites only slowly, releasing its calcium ion over tens of milliseconds, so that the sensor is primed for the calcium entry during a subsequent test impulse; this gives rise to F1 facilitation that decays with a time constant of ~50 ms. The idea that F1 facilitation does not arise as a consequence of residual calcium remaining in the terminal after the conditioning stimulus and is therefore likely to be due to a property of the calcium sensor protein is supported by a number of observations. F1 facilitation is unaffected by the calcium chelator bis-(aminophenoxy)ethane-tetraacetic acid (BAPTA) in crayfish motor nerve terminals (Winslow et al., 1994; but see Kamiya and Zucker, 1994, for the effect of photolabile calcium chelators removing F1 facilitation in this nerve terminal). The time course of decline in calcium in the region of the calcium sensor protein has been measured for the crayfish motor nerve terminal, using the current through calcium-activated potassium channels nearby as calcium detectors; this showed that the residual calcium in this region declines much faster than does F1 facilitation (Blundon et al., 1993). Finally, Robitaille and Charlton (1991) have argued on the basis of their BAPTA studies on the amphibian motor nerve terminal that residual calcium is not responsible for F1 facilitation, whereas Tanabe and Kijima (1992) have argued the opposite. Taken together, the evidence is not in favor of F1 facilitation being due to residual calcium, at least for the crayfish motor nerve terminal. In the present work, then, F1 facilitation has been ascribed to a property of two of the binding sites on the calcium sensor.

F2 facilitation, augmentation, and the calcium sensor protein

These observations and modeling suggest the properties that must be ascribed to at least two of the calcium-binding sites on the protein sensor, but what of the other two or more sites? Bertram et al. (1996) have argued that the remaining two sites should be given kinetic properties and affinities that allow these sites to determine the F2 phase of facilitation that lasts for ~500 ms and for augmentation that lasts for ~5 s. That is, these two binding sites should retain their calcium for times after a conditioning impulse that allow the priming of the protein sensor to decay along two exponentials with the time constants of F2 facilitation and augmentation. It seems unlikely that augmentation is due to a process of this kind rather than to the residual free calcium in the terminal that is left behind by the conditioning impulse. Such residual calcium, declining with a time constant of ~5 s, has been observed after stimulation to the mossy fibers ending on CA3 pyramidal neurons in the hippocampus (Regehr et al., 1994), the axons to the squid stellate ganglion (Swandulla et al., 1991), the crayfish motor nerve axon (Delaney and Tank, 1994), the parasympathetic nerves to the avian ciliary ganglion (Brain and Bennett, 1995), and the sympathetic nerves to the mouse vas deferens (Brain and Bennett, 1997). Furthermore, the introduction of various calcium chelating agents into the crayfish motor nerve terminal alters augmentation in a way that parallels that which occurs to the residual calcium at this time (Delaney and Tank, 1994). One caveat to the proposal that augmentation is due to residual calcium is provided by observations on amphibian motor nerve terminal that the calcium chelator BAPTA does not affect augmentation (Tanabe and Kijima, 1992). In the present work the affinities on the calcium sensor protein have not been adjusted to account for augmentation.

The question of whether the F2 phase of facilitation arises as a consequence of the properties of a binding site on the calcium sensor protein is more difficult to resolve. One of the components of decline of residual calcium after an impulse has the time course of F2 facilitation in Schaeffer collaterals to CA1 pyramidal neurons in the hippocampus (Wu and Saggau, 1994), in parasympathetic nerve terminals on avian ciliary ganglion cells (Brain and Bennett, 1995), and in sympathetic nerve terminals to the mouse vas deferens (Brain and Bennett, 1997). However, Delaney and Tank (1994) were unable to find residual calcium in crayfish

motor nerve terminals with the time course of F2 facilitation, and introduction of the calcium chelator BAPTA into this terminal does not affect F2 facilitation (see figure 3 in Winslow et al., 1994). Set against these results is the observation of Kamiya and Zucker (1994) that photolabile calcium chelators in the crayfish motor nerve terminal remove F2 facilitation, indicating that it is due to the removal of residual calcium, perhaps that observed by Tank et al. (1995). BAPTA has been reported to have no effect on F2 facilitation at amphibian motor nerve terminals (Tanabe and Kijima, 1992). It may be that F2 facilitation has its origins in both a residual component of calcium as well as in the properties of one of the binding sites on the calcium sensor protein, with some terminals possessing little residual calcium sequestered with the time course of F2 facilitation. Given this degree of uncertainty, the affinities of the calcium sensor have not been adjusted in the present work to account for F2 facilitation.

The calcium sensor protein in chromaffin cells

A quantitative analysis of secretion from chromaffin cells indicates that this can be described by a process involving three calcium noncooperative binding steps that have a K_d of 7–13 μM, that is about the K_d for synaptotagmin 1 calcium-dependent phospholipid binding of 7 μM (Table 2; Brose et al., 1992; Bazbek et al., 1995). Calcium-dependent phospholipid binding using the C2a domain of synaptotagmins 1, 2, or 3 could mediate this effect (Südhof, 1995). On the other hand, it could be restricted to the calcium-dependent syntaxin binding using the C2a domain of synaptotagmin 3. In any case, the secretion process involves a relatively high-affinity binding site that may well suit the relatively slow secretion process in these cells compared with nerve terminals that require a fast process that terminates quickly. It may be that the slow process of secretion from chromaffin cells is more akin to the slow component of increased probability that follows a nerve impulse in a terminal and is dependent on synaptotagmin 3. Quantal release from the terminals of goldfish retinal bipolar cells can also be described by a scheme analogous to that used to describe secretion from chromaffin cells, with in this case four calcium cooperative binding steps; the dissociation constant for one of the calcium-mediated bindings must have a K_d of ~143 μM rather than the much lower K_d of 7–13 μM used for chromaffin secretion (Table 2; Heildeberger et al., 1994). The inclusion of a low-affinity binding step (K_d of 143 μM), together with high-affinity steps (K_d of 9 μM), is required for the quantitative description of release, so that the kinetic scheme provides a fast turn-on, fast turn-off, and fast decay of quantal release. Previous theoretical studies have anticipated these experimental results. Thus Yamada and Zucker (1992) showed the necessity of including a rapidly equilibrating low-affinity calcium-binding site on the calcium sensor protein (with a K_d of 200 μM), as well as a slowly equilibrating high-affinity site (with a K_d of 1 μM). Similar ranges of K_d values have been used for multiple binding sites on the calcium sensor when calcium-mediated quantal release in the stellate ganglion of the squid was modeled (Bertram et al., 1996).

Exocytosis and the temperature dependence of release at active zones

The necessity of including an exocytosis step in models of quantal release to introduce an appropriate temperature dependence into the release process (Datyner and Gage, 1980) was first pointed out by Parnas et al. (1989). This irreversible process was given a forward rate constant of 1000 s^{-1}, a value that was subsequently found to give a good description of the exocytotic process in both chromaffin cells and the terminals of retinal bipolar cells (see Table 1; Heinemann et al., 1994; Heidelberger et al., 1994). In the present work the rate constant for the exocytotic step has been taken as 2000 s^{-1}.

Predictions of the synaptosecretosome model of release at active zones

The present analysis shows that the highest rate of exocytosis occurs after both the peak of the nerve impulse and the peak of the calcium concentration at the synaptosecretosome, as is observed experimentally in the squid stellate ganglion (Llinás et al., 1982). After the peak rate of exocytosis, there is a continuing elevated probability of release that lasts for tens of milliseconds or so, as a consequence of the occupation by calcium ions of the high-affinity binding sites on the calcium sensor protein. Thus the spontaneous opening of a calcium channel at this time (see Bennett et al., 1995) will more probably lead to the release of transmitter due to the calcium priming of the sensor; such enhanced spontaneous release is observed experimentally at the motor endplate (Rahamimoff and Yaari, 1973). The present analysis also shows how F1 facilitation decreases with an increase in the calcium concentration, as is observed experimentally at the endplate (Rahamimoff, 1968).

The present analysis shows that there is an invariance in the normalized time course of the rate of exocytosis after an impulse with large changes in the number of quanta released. This is the case whether it is due to changes in the calcium concentration and thus to the entry of calcium ions into the synaptosecretosome; a decrease in calcium entry into the terminal as a consequence of a decrease in the probability of calcium channel opening; or after a conditioning impulse, as in facilitation. Such an invariance in the time course of the rate of exocytosis has been observed experimentally after an increase in external calcium concentration (Datyner and Gage, 1980), as well as after the application of the autoreceptor agent adenosine (Van der Kloot, 1988), which most likely acts to decrease the probability of opening of the calcium channel (Bennett and Ho,

1991; Yawo and Chuhma, 1993), and during facilitation (Datyner and Gage, 1980).

The present theory also accounts for the relatively high incidence of evoked multiquantal secretion at sympathetic varicosities compared with that at the active zones of endplates (Bennett, 1994), as well as the level of quantal release observed at these junctions in normal calcium concentrations. The synaptosecretosome hypothesis also provides a basis for the linear relationship between the size of active zones and the probability of quantal secretion (Bennett et al., 1989), as probability increases with an increase in the number of synaptosecretosomes at an active zone according to the binomial equation. The variability in the probability of quantal release at the active zones of adjacent sympathetic varicosities (Lavidis and Bennett, 1993) and at adjacent active zones of motor endplates (Bennett et al., 1986; Zefirov et al., 1995) is therefore most likely due to variations in the number of synaptosecretosomes at these sites. The fourth-power dependence of this probability on the external calcium concentration is the same at the active zones of varicosities and endplates, independent of their probability in a particular calcium concentration (Bennett and Lavidis, 1989; MacLeod et al., 1994); this is the case according to the present theory.

The problem of nonindependence of synaptosecretosomes at active zones

The analysis presented in this work has treated the synaptosecretosomes as acting independently on the arrival of an impulse in the nerve terminal. In this case there is no overlap in calcium domains of different synaptosecretosomes. It follows that the probability of different numbers of quanta being released at an active zone is independent of the active zone structure and merely depends on the total number of synaptosecretosomes present at the active zones. In this case there is no qualitative difference between release at the active zones of varicosities, boutons, or endplates. An increase in the size of an active zone, whether organized into a line of synaptosecretosomes as at the endplate, a rectangular grid of synaptosecretosomes as in boutons, or a random array of synaptosecretosomes as in the case of varicosities, will simply lead to an increase in the probability of 0, 1, 2, etc., releases according to application of the binomial equation in which n is the total number of synaptosecretosomes in the terminal and p is their average probability of release. Neither the difficult problem of describing what happens if the calcium domains of synaptosecretosomes can overlap nor the problem of what happens if there is an excess of voltage-activated calcium channels over synaptosecretosomes has been considered in the present work. Indeed, there is evidence at the calyx synapse of the rat medial nucleus that several such channels must open for an exocytotic event to occur (Borst and Sakmann, 1996), although this does not seem to be the case for the motor endplate, for synapses in the squid stellate ganglion, or for the calyx synapse in the chick ciliary ganglion, as mentioned in the Introduction. An important point not yet considered is that although it seems likely that the N-type calcium channels at a synapse are complexed with syntaxin in the synaptosecretosome (el Far et al., 1995), as are the P/Q-type calcium channels in the synaptosecretosomes of those terminals that use these channels for triggering exocytosis (Martin-Moutot et al., 1996), it is still possible that there is an excess of syntaxin occurs in the presynaptic terminal membrane over that of N-type or P/Q-type calcium channels or vice versa. If there is an excess of calcium channels over syntaxin, then it will be necessary to consider the problem of synaptosecretosomes themselves occasionally coming into close proximity to these excess calcium channels (for an analogous case involving spontaneous quantal release, see figure 3 in Bennett et al., 1995).

APPENDIX: EQUATIONS FOR CALCIUM BINDING

Single-affinity scheme

For the single-affinity binding scheme described by Eq. 11, standard techniques (Feller, 1950, Ch. 17) give the following set of coupled differential equations for the probabilities:

$$\begin{aligned}
\frac{dP_0}{dt} &= -4\mu_1 P_0 + \nu_1 P_1 \\
\frac{dP_1}{dt} &= 4\mu_1 P_0 - (3\mu_2 + \nu_1)P_1 + 2\nu_2 P_2 \\
\frac{dP_2}{dt} &= 3\mu_2 P_1 - (2\mu_3 + 2\nu_2)P_2 + 3\nu_3 P_3 \\
\frac{dP_3}{dt} &= 2\mu_3 P_2 - (3\nu_3 + \mu_4)P_3 + 4\nu_4 P_4 \\
\frac{dP_4}{dt} &= \mu_4 P_3 - (4\nu_4 + \beta)P_4 \\
\frac{dP_{ex}}{dt} &= \beta P_4
\end{aligned} \tag{19}$$

with initial conditions

$$P_0(0) = 1; \quad P_k(0) = 0; \quad k \geq 1; \quad P_{ex}(0) = 0 \tag{20}$$

Double-affinity scheme

For the double-affinity binding scheme described by Eq. 13, the equations are

$$\begin{aligned}
\frac{dP_0}{dt} &= -(2\mu_L + 2\mu_H)P_0 + \nu_L P_L + \nu_H P_H \\
\frac{dP_L}{dt} &= 2\mu_L P_0 - (2\mu_H + \mu_L + \nu_L)P_L \\
&\quad + \nu_H P_{L+H} + 2\nu_L P_{2L}
\end{aligned}$$

$$\frac{dP_H}{dt} = 2\mu_H P_0 - (2\mu_L + \mu_H + \nu_L)P_H + \nu_L P_{H+L} + 2\nu_H P_{2H}$$

$$\frac{dP_{H+L}}{dt} = 2\mu_H P_L + 2\mu_L P_H - (\mu_L + \mu_H + \nu_L + \nu_H)P_{H+L} + 2\nu_L P_{2L+H} + 2\nu_H P_{2H+L}$$

$$\frac{dP_{2L}}{dt} = \mu_L P_L - (2\mu_H + 2\nu_L)P_{2L} + \nu_H P_{2L+H}$$

$$\frac{dP_{2H}}{dt} = \mu_H P_H - (2\mu_L + 2\nu_H)P_{2H} + \nu_L P_{2H+L}$$

$$\frac{dP_{2H+L}}{dt} = \mu_H P_{L+H} + 2\mu_L P_{2H} - (2\nu_H + \nu_L + \mu_L)P_{2H+L} + 2\nu_L P_{2H+2L}$$

$$\frac{dP_{2L+H}}{dt} = \mu_L P_{H+L} + 2\mu_H P_{2L} - (2\nu_L + \nu_H + \mu_H)P_{2L+H} + 2\nu_H P_{2L+2H}$$

$$\frac{dP_{2L+2H}}{dt} = \mu_L P_{2H+L} + \mu_H P_{2L+H} - \beta P_{2H+2L} - (2\nu_L + 2\nu_H)P_{2H+2L}$$

$$\frac{dP_{ex}}{dt} = \beta P_{2H+2L} \qquad (21)$$

with initial conditions

$$P_0(0) = 1; \quad P_k(0) = 0 \text{ in all other cases} \qquad (22)$$

Note that $P_{H+L} = P_{L+H}$, $P_{2H+2L} = P_{2L+2H}$, and P_{ex} is the probability of the state with all four sites occupied after a conformational change. The total probabilities of k sites occupied, $k = 1, \ldots, 4$, are P_k, where

$$\begin{aligned} P_1 &= P_L + P_H \\ P_2 &= P_{L+H} + P_{2L} + P_{2H} \\ P_3 &= P_{2L+H} + P_{2H+L} \\ P_4 &= P_{2H+2L} \end{aligned} \qquad (23)$$

In the case where $\mu_H = \mu_L = \mu$ and $\nu_H = \nu_L = \nu$, Eqs. 21 and 23 reduce to Eq. 19, with $\mu_i = \mu$, $\nu_i = \nu$, $i = 1, \ldots, 4$.

We thank Nathan Bylett and Jon Turner for assistance with computing.

This work was supported by Australian Research Council grant AC9330365.

REFERENCES

Aharon, S., H. Parnas, and I. Parnas. 1994. The magnitude and significance of Ca^{2+} domains for release of neurotransmitter. *Bull. Math. Biol.* 56:1095–1119.

Augustine, G. J., E. M. Adler, and M. P. Charlton. 1991. The calcium signal for transmitter secretion from presynaptic nerve terminals. *Ann. N.Y. Acad. Sci.* 635:365–381.

Augustine, G. J., M. P. Charlton, and S. J. Smith. 1985. Calcium entry and transmitter release at voltage-clamped nerve terminals of squid. *J. Physiol. (Lond.).* 367:163–181.

Bazbek, C. L., B. A. Davletov, and T. C. Südhof. 1995. Distinct Ca^{2+} and Sr^{2+} binding sites of synaptotagmins. *J. Biol. Chem.* 270:24898–24902.

Bennett, M. R. 1994. Quantal secretion from single visualized synaptic varicosities of sympathetic nerve terminals. *Adv. Second Messenger Phosphoprotein Res.* 29:399–423.

Bennett, M. R., L. Farnell, W. G. Gibson, and N. A. Lavidis. 1997. Synaptic transmission at visualized sympathetic boutons: stochastic interaction between acetylcholine and its receptors. *Biophys. J.* 72:1595–1606.

Bennett, M. R., and C. Fisher. 1977. The effects of calcium ions on the binomial parameters that control acetylcholine release during trains of nerve impulses at amphibian neuromuscular synapses. *J. Physiol. (Lond.).* 271:673–698.

Bennett, M. R., W. G. Gibson, and J. Robinson. 1995. Probabilistic secretion of quanta: spontaneous release at active zones of varicosities, boutons and endplates. *Biophys. J.* 69:42–53.

Bennett, M. R., and S. Ho. 1991. Probabilistic secretion of quanta from nerve terminals in avian ciliary ganglia modulated by adenosine. *J. Physiol. (Lond.).* 440:513–527.

Bennett, M. R., P. Jones, and N. A. Lavidis. 1986. The probability of quantal secretion along visualized terminal branches at amphibian (*Bufo marinus*) neuromuscular synapses. *J. Physiol. (Lond.).* 379:257–274.

Bennett, M. R., S. Karunanithi, and N. A. Lavidis. 1991. Probabilistic secretion of quanta from nerve terminals in toad (*Bufo marinus*) muscle modulated by adenosine. *J. Physiol. (Lond.).* 433:421–434.

Bennett, M. R., N. A. Lavidis, and F. Lavidis-Armson. 1989. The probability of quantal secretion at release sites of different length in toad (*Bufo marinus*) muscle. *J. Physiol. (Lond.).* 418:235–249.

Bertram, R., A. Sherman, and E. F. Stanley. 1996. Single-domain/bound calcium hypothesis of transmitter release and facilitation. *J. Neurosci.* 75:1919–1931.

Blundon, J. A., S. N. Wright, M. S. Brodwick, and G. D. Bittner. 1993. Presynaptic calcium-activated potassium channels and calcium channels at a crayfish neuromuscular junction. *J. Neurophysiol.* 73:178–189.

Borst, J. G. G., and B. Sakmann. 1996. Calcium influx and transmitter release in a fast CNS synapse. *Nature* 383:431–434.

Brain, K. L., and M. R. Bennett. 1995. Calcium in the nerve terminals of chick ciliary ganglia during facilitation, augmentation and potentiation. *J. Physiol. (Lond.).* 489:637–648.

Brain, K. L., and M. R. Bennett. 1997. Calcium in sympathetic varicosities of mouse vas deferens during facilitation, augmentation and autoinhibition. *J. Physiol. (Lond.).* 1502:521–536.

Brinley, F. J. 1978. Calcium buffering in squid axons. *Annu. Rev. Biophys. Bioeng.* 7:363–392.

Brose, N., A. G. Petrenko, T. C. Südhof, and R. Jahn. 1992. Synaptotagmin: a calcium sensor on the synaptic vesicle surface. *Science.* 256:1021–1025.

Clay, J. R., and L. J. DeFelice. 1983. Relationship between membrane excitability and single channel open-close kinetics. *Biophys. J.* 42: 151–157.

Datyner, N. B., and P. W. Gage. 1980. Phasic secretion of acetylcholine at a mammalian neuromuscular junction. *J. Physiol. (Lond.).* 303:299–314.

Delaney, K. R., and D. W. Tank. 1994. A quantitative measurement of the dependence of short-term synaptic enhancement on presynaptic residual calcium. *J. Neurosci.* 14:5885–5902.

Delcour, A. H., D. Lipscombe, and R. W. Tsien. 1993. Multiple modes of N-type calcium channel activity distinguished by differences in gating kinetics. *J. Neurosci.* 13:181–194.

Dodge, F. A., and R. Rahamimoff. 1967. Co-operative action of calcium ions in transmitter release at the neuromuscular junction. *J. Physiol. (Lond.).* 193:419–432.

el Far, O., N. Charvin, C. Leveque, N. Martin-Moutot, M. Takahashi, and M. J. Seagar. 1995. Interaction of synaptobrevin (VAMP)-syntaxin complex with presynaptic calcium channels. *FEBS Lett.* 361:101–105.

Feller, W. 1950. An Introduction to Probability Theory and its Applications, Vol. 1, 3rd Ed. Wiley, New York.

Fogelson, A. L., and R. S. Zucker. 1985. Presynaptic calcium diffusion from various arrays of single channels: implications for transmitter release and synaptic facilitation. *Biophys. J.* 48:1003–1017.

Haydon, P. G., E. Henderson, and E. F. Stanley. 1994. Localization of individual calcium channels at the release face of a presynaptic nerve terminal. *Neuron.* 13:1275–1280.

Heidelberger, R., C. Heinemann, E. Neher, and G. Matthews. 1994. Calcium dependence of the rate of exocytosis in a synaptic terminal. *Nature.* 371:513–515.

Heinemann, C., R. H. Chow, E. Neher, and R. S. Zucker. 1994. Kinetics of the secretory response in bovine chromaffin cells following flash photolysis of caged calcium. *Biophys. J.* 67:2546–2557.

Hille, B. 1992. Ionic Channels of Excitable Membranes. Sinauer Associates, Sunderland, MA.

Jones, W. W., and T. N. Marks. 1989a. Calcium currents in bullfrog sympathetic neurons. I. Activation kinetics and pharmacology. *J. Gen. Physiol.* 94:151–167.

Jones, W. W., and T. N. Marks. 1989b. Calcium currents in bullfrog sympathetic neurons. II. Inactivation. *J. Gen. Physiol.* 94:169–182.

Kamiya, H., and R. S. Zucker. 1994. Residual Ca^{2+} and short-term synaptic plasticity. *Nature.* 371:603–606.

Katz, B., P. A. Ferro, B. D. Cherksey, M. Sugimori, R. Llinás, and O. D. Uchitel. 1995. Effect of Ca^{2+} channel blockers on transmitter release and presynaptic currents at the frog neuromuscular junction. *J. Physiol. (Lond.).* 486:695–706.

Lavidis, N. A., and M. R. Bennett. 1993 Probabilistic secretion of quanta from visualized varicosities along single sympathetic nerve terminals. *J. Auton. Nerv. Syst.* 43:41–50.

Llinás, R., I. Z. Steinberg, and K. Walton. 1981. Relationship between presynaptic calcium current and postsynaptic potential in squid giant synapse. *Biophys. J.* 33:323–352.

Llinás, R., M. Sugimori, and R. B. Silver. 1995. Time resolved calcium microdomains and synaptic transmission. *J. Physiol. (Paris).* 89:77–81.

Llinás, R., M. Sugimori, and S. M. Simon. 1982. Transmission by presynaptic spike-like depolarization in the squid giant synapse. *Proc. Natl. Acad. Sci. USA.* 79:2415–2419.

MacLeod, G., N. A. Lavidis, and M. R. Bennett. 1994. Calcium dependence of quantal secretion from visualized sympathetic nerve varicosities on the mouse vas deferens. *J. Physiol. (Lond.).* 480:61–70.

Magleby, K. L., and D. C. Miller. 1982. Facilitation, augmentation, and potentiation of transmitter release. *Prog. Brain Res.* 49:175–182.

Martin-Moutot, N., N. Charvin, C. Leveque, K. Sato, T. Nishiki, S. Kozaki, M. Takahashi, and M. Seagar. 1996. Interaction of SNARE complexes with P/Q-type calcium channels in rat cerebellar synaptosomes. *J. Biol. Chem.* 271:6567–6570.

O'Connor, V. M., O. Shamotienko, E. Grishin, and H. Betz. 1993. On the structure of the "synaptosecretosome." Evidence for a neurexin/synaptotagmin/syntaxin/Ca^{2+} channel complex. *FEBS Lett.* 326: 255–260.

Parnas, H., G. Hovav, and I. Parnas. 1989. Effect of Ca^{2+} diffusion on the time course of neurotransmitter release. *Biophys. J.* 55:859–874.

Rahamimoff, R. 1968. A dual effect of calcium ions on neuromuscular facilitation. *J. Physiol. (Lond.).* 195:471–480.

Rahamimoff, R., and Y. Yaari. 1973. Delayed release of transmitter at the frog neuromuscular junction. *J. Physiol. (Lond.).* 228:241–257.

Regehr, W. G., K. R. Delaney, and D. W. Tank. 1994. The role of presynaptic calcium in short-term enhancement at the hippocampal mossy fiber synapse. *J. Neurosci.* 14:523–537.

Robitaille, R., and M. P. Charlton. 1991. Frequency facilitation is not caused by residual ionised calcium at the frog neuromuscular junction. *Ann. N.Y. Acad. Sci.* 635:492–494.

Simon, S. M., and R. R. Llinás. 1985. Compartmentalization of the submembrane calcium activity during calcium influx and its significance in transmitter release. *Biophys. J.* 48:485–498.

Stanley, E. F. 1993. Single calcium channels and acetylcholine release at a presynaptic nerve terminal. *Neuron.* 11:1007–1011.

Südhof, T. C. 1995. The synaptic vesicle cycle: a cascade of protein-protein interactions. *Nature.* 375:645–653.

Swandulla, D., M. Hans, K. Zipser, and G. J. Augustine. 1991. Role of residual calcium in synaptic depression and posttetanic potentiation: fast and slow calcium signaling in nerve terminals. *Neuron.* 7:915–926.

Tanabe, N., and H. Kijima. 1992. Ca(2+)-dependent and -independent components of transmitter release at the frog neuromuscular junction. *J. Physiol. (Lond.).* 455:271–289.

Tank, D. W., W. G. Regehr, and K. R. Delaney. 1995. A quantitative analysis of presynaptic calcium dynamics that contribute to short-term enhancement. *J. Neurosci.* 15:7940–7952.

Thompson, P. C., N. A. Lavidis, J. Robinson, and M. R. Bennett. 1995. Probabilistic secretion of quanta at somatic motor-nerve terminals: the fusion-pore model, quantal detection and autoinhibition. *Philos. Trans. R. Soc. Lond. B.* 349:197–214.

Van der Kloot, W. 1988. Estimating the timing of quantal releases during end-plate currents at the frog neuromuscular junction. *J. Physiol. (Lond.).* 402:595–603.

Winslow, J. L., S. N. Duffy, and M. P. Charlton. 1994. Homosynaptic facilitation of transmitter release in crayfish is not affected by mobile calcium chelators: implications for the residual ionized calcium hypothesis from electrophysiological and computational analyses. *J. Neurophysiol.* 72:1769–1793.

Wright, C. E., and J. A. Angus. 1996. Effects of n-, p- and q-type neuronal calcium channel antagonists on mammalian peripheral neurotransmission. *Br. J. Pharmacol.* 119:49–56.

Wu, L. G., and P. Saggau. 1994. Presynaptic calcium is increased during normal synaptic transmission and paired-pulse facilitation but not in long-term potentiation in area CA1 of hippocampus. *J. Neurosci.* 14: 645–654.

Yamada, W. M., and R. S. Zucker. 1992. Time course of transmitter release calculated from simulations of a calcium diffusion model. *Biophys. J.* 61:671–682.

Yawo, H., and N. Chuhma. 1993. Preferential inhibition of omega-conotoxin-sensitive presynapitic Ca^{2+} channels by adenosine autoreceptors. *Nature.* 365:256–258.

Yoshida, A., C. Oho, A. Omore, R. Kuwahara, T. Ito, and M. Takahashi. 1992. HPC-1 is associated with synaptotagmin and omega-conotoxin receptor. *J. Biol. Chem.* 267:24925–24928.

Yoshikami, D., Z. Bagaboldo, and B. M. Olivera. 1989. The inhibitory effects of omega-conotoxins on Ca channels and synapses. *Ann. N.Y. Acad. Sci.* 560:230–248.

Zefirov, A., T. Benish, N. Fatkullin, S. Cheranov, and R. Khazipov. 1995. Localization of active zones. *Nature.* 376:393–394.

Zucker, R. S., and A. L. Fogelson. 1986. Relationship between transmitter release and presynaptic calcium influx when calcium enters through discrete channels. *Proc. Natl. Acad. Sci. USA.* 83:3032–3036.